Pendant-functionalised Ligands for Metallosupramolecular Assemblies; Ruthenium(II) and Osmium(II) Complexes of 4'-(4-Pyridyl)-2,2':6',2"-terpyridine†

Edwin C. Constable[*,a,b] **and Alexander M. W. Cargill Thompson**[a,b]

[a] *Institut für Anorganische Chemie, Universität Basel, Spitalstrasse 51, CH-4056 Basel, Switzerland*

[b] *Cambridge Centre for Molecular Recognition, University Chemical Laboratory, Lensfield Road, Cambridge CB2 1EW, UK*

The potentially tetradentate ligand 4'-(4-pyridyl)-2,2':6',2"-terpyridine (pyterpy) acts as a tridentate donor to iron(II), ruthenium(II) and osmium(II). The non-co-ordinated pyridyl group reacts with a range of electrophiles to give complexes containing the cationic ligands Hpyterpy and 4'-(4-methylpyridinio)-2,2':6',2"-terpyridine (mpyterpy). The electrochemical behaviour of these complexes has been studied and correlations between the redox potentials and Hammett σ^+ parameters made.

We are currently exploring the use of multi-domain ligands for the controlled assembly of metallosupramolecular architectures.[1-3] Metallosupramolecules are assembled from the interaction of metal ions with appropriate multifunctional ligands; the assembly process is coded by the acceptor properties of the metal ions (size, co-ordination number and co-ordination geometry) and the donor properties of the ligand (number and spatial arrangement of donor atoms).[1] Ligands containing two or more discrete metal-binding domains are of particular importance in this area, since they may be used subtly to control the spatial consequences of the assembly process. This philosophy has been applied to the synthesis of a variety of novel unnatural products. In our studies of metal-directed helication processes we became aware of the high degree of selectivity which could be achieved by the use of two or more *different* metal-binding domains within a given ligand.[2] We have recently described the preparation and reaction with electrophiles of iron(II) complexes of the ligand 4'-(4-pyridyl)-2,2':6',2"-terpyridine (pyterpy), which contains spatially separated tri- and mono-dentate domains.[4] In this paper we describe some redox-active ruthenium(II) and osmium(II) mononuclear complexes of pyterpy.

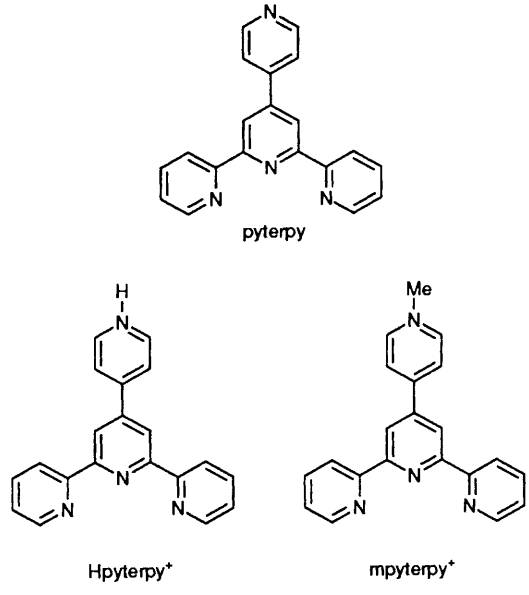

Experimental

Proton NMR spectra were recorded on a Brüker WM250 spectrometer, fast atom bombardment (FAB) mass spectra on a Kratos MS-890 spectrometer, using 3-nitrobenzyl alcohol as matrix. Electrochemical measurements were performed using an AMEL model 553 potentiostat, model 567 function generator and model 721 integrator connected to an X–Y recorder *via* an AMEL model 560/A interface. A conventional three-electrode configuration was used, with platinum-bead working and auxiliary electrodes and an $Ag–Ag^+$ reference. Acetonitrile, freshly distilled from P_4O_{10}, was used as solvent in all cases. The base electrolyte was 0.1 mol dm^{-3} $[NBu^n_4][BF_4]$, recrystallised twice from ethanol–water and thoroughly dried. Potentials are quoted *vs.* the ferrocene–ferrocenium couple (0.0 V), and all potentials were referenced to internal ferrocene added at the end of each experiment. Elemental analyses were performed at the University Chemical Laboratory, Cambridge.

Hydrated ruthenium(III) chloride and $Na_2[OsCl_6]$ were used as supplied by Johnson Matthey. The ligand 4'-(4-pyridyl)-2,2':6',2"-terpyridine (pyterpy)[4] and the complexes $[Ru(pterpy)Cl_3]$ (pterpy = 4'-phenyl-2,2':6',2"-terpyridine),[6] $[Ru(terpy)_2][PF_6]_2$,[6] and $[Os(terpy)_2][PF_6]_2$[7] were prepared as described elsewhere.

Preparations.—$[Ru(pyterpy)Cl_3]$. A suspension of $RuCl_3 \cdot 3H_2O$ (0.078 g, 0.323 mmol) and 4'-(4-pyridyl)-2,2':6',2"-terpyridine (0.100 g, 0.323 mmol) in ethanol (20 cm^3) was heated at reflux for 3 h. After this time the dark brown precipitate which had formed was filtered off and air dried to give $[Ru(pyterpy)Cl_3]$ (0.130 g, 78%).

$[Ru(pterpy)(pyterpy)][PF_6]_2$. (*i*) The complex $[Ru(pterpy)Cl_3]$ (0.100 g, 0.194 mmol) and pyterpy (0.060 g, 0.194 mmol) were suspended in methanol (10 cm^3). *N*-Ethylmorpholine (5 drops) was added, and the mixture heated at reflux for 2 h. After this time the resulting dark solution was allowed to cool, and an excess of methanolic $[NH_4][PF_6]$ added. The dark brown precipitate that formed was collected on Celite by filtration, and then redissolved in acetonitrile for chromatography on silica. A short column of silica (15 cm long, 3 cm wide) was used,

† *Non-SI unit employed:* eV ≈ 1.60 × 10^{-19} J.

with acetonitrile–saturated aqueous potassium nitrate–water (7:1:0.5 v/v) as eluent. The third, major, red-orange fraction was collected, an excess of methanolic $[NH_4][PF_6]$ added, and the solution reduced in volume to precipitate $[Ru(pterpy)(pyterpy)]^{2+}$ as the hexafluorophosphate salt. Recrystallisation from acetone–methanol (1:1) afforded $[Ru(pterpy)(pyterpy)][PF_6]_2$ as a red-brown powder (0.050 g, 25%). FAB (^{102}Ru) mass spectrum: *m/z* 866 (866) $[M - PF_6]^+$ and 721 (721) $[M - 2PF_6]^+$.

(*ii*) The complex $[Ru(pyterpy)Cl_3]$ (0.020 g, 0.038 mmol) and pterpy (0.012 g, 0.038 mmol) were suspended in methanol (10 cm^3). *N*-Ethylmorpholine (5 drops) was added, and the mixture heated at reflux for 2 h. No reaction was observed to have occurred after this time, the $[Ru(pyterpy)Cl_3]$ remaining undissolved. Still no reaction had occurred after 24 h at reflux.

$[Ru(pterpy)(mpyterpy)][PF_6]_3$ [mpyterpy = 4′-(4-*methylpyridinio*)-2,2′:6′,2″-*terpyridine*]. The complex $[Ru(pterpy)Cl_3]$ (0.100 g, 0.194 mmol) and pyterpy (0.060 g, 0.194 mmol) were suspended in methanol (10 cm^3). *N*-Ethylmorpholine (5 drops) was added, and the mixture heated at reflux for 2 h. After this time, methyl iodide (1 cm^3, excess) was added to the resulting solution, which was then heated at reflux for 2 h. The dark solution was allowed to cool, and an excess of methanolic $[NH_4][PF_6]$ added. The dark brown precipitate formed was collected on Celite by filtration, and then redissolved in acetonitrile for chromatography on silica. A short column of silica (15 cm long, 3 cm wide) was used, with acetonitrile–saturated aqueous potassium nitrate–water (7:1:0.5 v/v) as eluent. The major brown fraction was collected, an excess of methanolic $[NH_4][PF_6]$ added, and the solution reduced in volume to precipitate $[Ru(pterpy)(mpyterpy)]^{3+}$ as the hexafluorophosphate salt. Recrystallisation from acetone–methanol (1:1) afforded $[Ru(pterpy)(mpyterpy)][PF_6]_3$ as a red-brown powder (0.035 g, 18%) (Found: C, 41.7; H, 2.6; N, 8.1. $C_{42}H_{32}F_{18}N_7P_3Ru$ requires C, 43.1; H, 2.7; N, 8.4%). FAB (^{102}Ru) mass spectrum: *m/z* 1027 (1026) $[M - PF_6]^+$, 881 (881) $[M - 2PF_6]^+$, 736 (736) $[M - 3PF_6]^+$ and 721 (721) $[M - Me - 3PF_6]^+$.

$[Ru(pyterpy)_2][PF_6]_2$. (*i*) A suspension of $[Ru(pyterpy)Cl_3]$ (0.062 g, 0.120 mmol) and pyterpy (0.037 g, 0.120 mmol) in methanol (10 cm^3) was heated at reflux for 4 h. No reaction was observed to have occurred after this time, nor after 20 h at reflux, the dark brown $[Ru(pyterpy)Cl_3]$ remaining undissolved.

(*ii*) A suspension of $RuCl_3 \cdot 3H_2O$ (0.019 g, 0.079 mmol) and pyterpy (0.049 g, 0.158 mmol) in ethane-1,2-diol (10 cm^3) was heated at reflux for 3 h. After this time the mixture was allowed to cool, and water (10 cm^3) and an excess of methanolic $[NH_4][PF_6]$ were added. The resulting dark brown precipitate was collected on Celite by filtration, and then redissolved in acetonitrile. The acetonitrile solution was reduced to minimum volume, and chromatographed on a short silica column (15 cm long, 3 cm wide), using acetonitrile–saturated aqueous potassium nitrate–water (7:1:0.5 v/v) as eluent. The first major orange fraction was collected, an excess of methanolic $[NH_4][PF_6]$ added, and the solution reduced in volume to precipitate $[Ru(pyterpy)_2]^{2+}$ as the hexafluorophosphate salt. Recrystallisation from acetone–methanol (1:1) afforded $[Ru(pyterpy)_2][PF_6]_2$ as a red-brown microcrystalline solid (0.048 g, 60%) (Found: C, 47.2; H, 2.7; N, 11.1. $C_{40}H_{28}F_{12}N_8P_2Ru$ requires C, 47.5; H, 2.8; N, 11.1%). FAB (^{102}Ru) mass spectrum: *m/z* 867 (867) $[M - PF_6]^+$ and 722 (722) $[M - 2PF_6]^+$.

$[Ru(Hpyterpy)_2][PF_6]_4$. A solution of $[Ru(pyterpy)_2][PF_6]_2$ (0.020 g, 0.020 mmol) in acetone (25 cm^3) and methanol (25 cm^3) was treated with HPF_6 (10 drops). The colour immediately changed from orange to pink. The solution was reduced in volume to precipitate a red-brown powder, which was filtered off, washed well with water and diethyl ether, and dried *in vacuo* giving $[Ru(Hpyterpy)_2][PF_6]_4$ (0.020 g, 78%). FAB (^{102}Ru) mass spectrum: *m/z* 1013 (1013) $[Ru(pyterpy)_2(PF_6)_2 + H]^+$, 867 (867) $[Ru(pyterpy)_2(PF_6)]^+$ and 722 (722) $[Ru(pyterpy)_2]^+$.

$[Ru(pyterpy)(mpyterpy)][PF_6]_3$ *and* $[Ru(mpyterpy)_2][PF_6]_4$. The complex $[Ru(pyterpy)_2][PF_6]_2$ (0.077 g, 0.076 mmol) was dissolved in acetonitrile (50 cm^3) by warming gently. A suspension of $[Me_3O][BF_4]$ (0.3 g, excess) in chloroform (20 cm^3) was added, and the mixture was heated at reflux for 30 min. The mixture was allowed to cool, and water (25 cm^3) and an excess of methanolic $[NH_4][PF_6]$ were added. Reduction in volume afforded a dark brown precipitate, which was collected on Celite by filtration and then redissolved in acetonitrile. The acetonitrile solution was reduced to minimum volume, and chromatographed on a short silica column (8 cm long, 3 cm wide), using acetonitrile–saturated aqueous potassium nitrate–water (7:1:0.5 v/v) as eluent. Three fractions were collected. The first minor orange fraction was unreacted $[Ru(pyterpy)_2]^{2+}$, which was discarded. The second, slower-moving, major brown fraction and the third, extremely slow moving, major pink fraction were collected and precipitated as hexafluorophosphate salts by addition of an excess of methanolic $[NH_4][PF_6]$ followed by reduction in volume. Recrystallisation of these two products from acetonitrile–water (1:1) afforded $[Ru(pyterpy)(mpyterpy)][PF_6]_3$ and $[Ru(mpyterpy)_2][PF_6]_4$, respectively. The monomethylated product $[Ru(pyterpy)(mpyterpy)][PF_6]_3$ was obtained as a red-brown powder (0.017 g, 19%) (Found: C, 40.4; H, 2.8; N, 9.5. $C_{41}H_{31}F_{18}N_8P_3Ru$ requires C, 42.0; H, 2.7; N, 9.6%). FAB (^{102}Ru) mass spectrum: *m/z* 1028 (1027) $[M - PF_6]^+$, 882 (882) $[M - 2PF_6]^+$, 737 (737) $[M - 3PF_6]^+$ and 722 (722) $[M - Me - 3PF_6]^+$. The bis(methylated) product $[Ru(mpyterpy)_2][PF_6]_4$ was obtained as a red-brown powder (0.034 g, 34%) (Found: C, 37.2; H, 2.4; N, 8.4. $C_{42}H_{34}F_{24}N_8P_4Ru$ requires C, 37.9; H, 2.6; N, 8.4%). FAB (^{102}Ru) mass spectrum: *m/z* 1187 (1187) $[M - PF_6]^+$, 1043 (1042) $[M - 2PF_6]^+$, 897 (897) $[M - 3PF_6]^+$, 752 (752) $[M - 4PF_6]^+$ and 736 (737) $[M - Me - 4PF_6]^+$.

$[Os(pyterpy)_2][PF_6]_2$. A suspension of $Na_2[OsCl_6]$ (0.070 g, 0.156 mmol) and 4′-(4-pyridyl)-2,2′:6′,2″-terpyridine (0.097 g, 0.312 mmol) in ethane-1,2-diol (10 cm^3) was heated at reflux for 2 h. The resulting mixture was allowed to cool, and water (10 cm^3) and an excess of methanolic $[NH_4][PF_6]$ were added. The resulting dark brown precipitate was collected on Celite by filtration and then redissolved in acetonitrile. The acetonitrile solution was reduced to minimum volume, and chromatographed on a short silica column (15 cm long, 3 cm wide), using acetonitrile–saturated aqueous potassium nitrate–water (7:1:0.5 v/v) as eluent. The first major brown fraction was collected, an excess of methanolic $[NH_4][PF_6]$ added, and the solution reduced in volume to precipitate $[Os(pyterpy)_2]^{2+}$ as the hexafluorophosphate salt. Recrystallisation from acetone–methanol (1:1) solution afforded $[Os(pyterpy)_2][PF_6]_2$ as a black microcrystalline solid (0.075 g, 44%) (Found: C, 43.7; H, 2.4; N, 10.5. $C_{40}H_{28}F_{12}N_8OsP_2$ requires C, 43.6; H, 2.5; N, 10.2%). FAB (^{192}Os) mass spectrum: *m/z* 958 (957) $[Os(pyterpy)_2(PF_6)]^+$ and 813 (812) $[Os(pyterpy)_2]^+$.

$[Os(Hpyterpy)_2][PF_6]_4$. A solution of $[Os(pyterpy)_2][PF_6]_2$ (0.032 g, 0.029 mmol) in acetonitrile (10 cm^3) and methanol (10 cm^3) was treated with HPF_6 (10 drops) in water (10 cm^3). The colour of the solution immediately changed from brown to purple. The solution was reduced in volume to precipitate a dark brown powder, which was filtered off, washed well with water and ether, and dried *in vacuo* giving $[Os(Hpyterpy)_2][PF_6]_4$ as a black powder (0.034 g, 84%) (Found: C, 33.9; H, 2.3; N, 8.2. $C_{40}H_{30}F_{24}N_8OsP_4$ requires C, 34.5; H, 2.2; N, 8.1%). FAB (^{192}Os) mass spectrum: *m/z* 1104 (1104) $[Os(pyterpy)_2(PF_6)_2 + 2H]^+$, 958 (958) $[Os(pyterpy)_2(PF_6) + H]^+$ and 813 (813) $[Os(pyterpy)_2 + H]^+$.

$[Os(pyterpy)(mpyterpy)][PF_6]_3$ *and* $[Os(mpyterpy)_2][PF_6]_4$. The complex $[Os(pyterpy)_2][PF_6]_2$ (0.045 g, 0.041 mmol) was dissolved in acetonitrile (50 cm^3) by warming gently. A suspension of $[Me_3O][BF_4]$ (0.2 g, excess) in chloroform (25 cm^3) was added, and the mixture heated at reflux for 30 min. The mixture was allowed to cool, and water (25 cm^3) and an

excess of methanolic $[NH_4][PF_6]$ were added. Reduction in volume afforded a dark brown precipitate, which was collected on Celite by filtration and then redissolved in acetonitrile. The acetonitrile solution was reduced to minimum volume, and chromatographed on a short silica column (8 cm long, 3 cm wide), using acetonitrile–saturated aqueous potassium nitrate–water (7:1:0.5 v/v) as eluent. Three fractions were collected. The first minor brown fraction was unreacted $[Os(pyterpy)_2]^{2+}$, which was discarded. The second, slower-moving, major purple-brown fraction and the third, extremely slow moving, major purple-brown fraction were collected and precipitated as hexafluorophosphate salts by addition of an excess of methanolic $[NH_4][PF_6]$ followed by reduction in volume. Recrystallisation of these two products from acetonitrile–water (1:1) afforded $[Os(pyterpy)(mpyterpy)][PF_6]_3$ and $[Os(mpyterpy)_2][PF_6]_4$, respectively. The monomethylated product $[Os(pyterpy)(mpyterpy)][PF_6]_3$ was obtained as a black powder (0.012 g, 23%) (Found: C, 37.2; H, 2.3; N, 8.8. $C_{41}H_{31}F_{18}N_8OsP_3$ requires C, 39.0; H, 2.5; N, 8.9%). FAB (^{192}Os) mass spectrum: m/z 1118 (1117) $[M - PF_6]^+$, 973 (972) $[M - 2PF_6]^+$, 826 (827) $[M - 3PF_6]^+$ and 811 (812) $[M - Me - 3PF_6]^+$. The bis(methylated) product $[Os(mpyterpy)_2][PF_6]_4$ was obtained as a black powder (0.012 g, 21%) (Found: C, 35.5; H, 2.3; N, 8.0. $C_{42}H_{34}F_{24}N_8OsP_4$ requires C, 35.5; H, 2.4; N, 7.9%). FAB (^{192}Os) mass spectrum: m/z 1278 (1277) $[M - PF_6]^+$, 1131 (1132) $[M - 2PF_6]^+$, 988 (987) $[M - 3PF_6]^+$, 839 (842) $[M - 4PF_6]^+$ and 826 (827) $[M - Me - 4PF_6]^+$.

Results and Discussion

The compound pyterpy is potentially a dinucleating tetradentate ligand, incorporating a tridentate 2,2′:6′,2″-terpyridine functionality, as well as an isolated monodentate pendant pyridyl group. The terpy moiety is ideal for tridentate coordination to d^6 metal centres to give chelation-stabilised complexes of the form $[M(pyterpy)_2]^{n+}$. We have demonstrated that, if a kinetically inert d^6 centre such as ruthenium(II), cobalt(III) or osmium(II) is present, such species may be used as building blocks for the assembly of co-ordination oligomers.[5] Each of the two pyterpy ligands in such a complex possesses a non-co-ordinated pendant pyridine group which can readily be protonated or alkylated to give a pyridinium salt, or co-ordinated to a second metal centre. The effect of any of these processes is to generate a molecule which may be regarded as a 2,2′:6′,2″-terpyridine with a significantly electron-withdrawing substituent, and this is expected to exert a profound effect upon the central d^6 metal centre.

We initially decided to prepare ruthenium(II) complexes of pyterpy. The preparation of $[Ru(pyterpy)_2]^{2+}$ salts proved to be less facile than that of $[Fe(pyterpy)_2]^{2+}$ derivatives, primarily due to the reduced lability of ruthenium(II) species compared to the iron(II) analogues. The mild, two-step, methodology that we have developed for the synthesis of homoleptic $[Ru(X\text{-terpy})_2]^{2+}$ and heteroleptic $[Ru(X\text{-terpy})(Y\text{-terpy})]^{2+}$ complexes (X-terpy, Y-terpy = 4′-substituted 2,2′:6′,2″-terpyridine)[6] proved to be unsuccessful. The crucial intermediates in this strategy are the 1:1 ruthenium(III) complexes $[Ru(X\text{-terpy})Cl_3]$ or $[Ru(Y\text{-terpy})Cl_3]$. The reaction of commercial hydrated ruthenium trichloride with 1 equivalent of pyterpy at reflux in methanol gave an insoluble, dark brown, powder which was assumed to be $[Ru(pyterpy)Cl_3]$. This product was not further characterised. As we[6] and others[7] have previously reported, the ruthenium(III) species $[Ru(X\text{-terpy})Cl_3]$ are extremely insoluble in a wide variety of organic solvents, and their purification and further characterisation is not usually pursued.

In contrast to the behaviour of all other $[Ru(X\text{-terpy})Cl_3]$ complexes that we have studied, $[Ru(pyterpy)Cl_3]$ did not undergo any reaction upon boiling with a solution of 1 equivalent of pyterpy in methanol in the presence of the reducing agent *N*-ethylmorpholine, even after prolonged reaction times. This observation may be indicative that the ruthenium(III) species $[Ru(pyterpy)Cl_3]$ is polymeric, with adjacent ruthenium centres being bridged by the pendant pyridyl moieties. In order to determine whether the low reactivity is an inherent property of the pyterpy ligand or is due to the nature of $[Ru(pyterpy)Cl_3]$, we attempted to prepare the heteroleptic complex cation $[Ru(pterpy)(pyterpy)]^{2+}$ (pterpy = 4′-phenyl-2,2′:6′,2″-terpyridine) by two complementary routes. These experiments confirmed that the failure of the initial attempt at the preparation of $[Ru(pyterpy)_2]^{2+}$ is associated with the nature of $[Ru(pyterpy)Cl_3]$, since $[Ru(pterpy)(pyterpy)]^{2+}$ could be prepared by the reaction of equimolar quantities of $[Ru(pterpy)Cl_3]$ with pyterpy at reflux in methanol in the presence of a reducing agent, but not by the alternative reaction of equimolar quantities of $[Ru(pyterpy)Cl_3]$ and pterpy. The dark brown, crude reaction mixture thus obtained was precipitated by the addition of an excess of methanolic $[NH_4][PF_6]$. The precipitate was collected and redissolved in the minimum volume of acetonitrile for column chromatography on silica, using acetonitrile–saturated aqueous potassium nitrate–water (7:1:0.5 v/v) as eluent. The third, major, red-orange fraction was collected, methanolic $[NH_4][PF_6]$ added, and the solution reduced in volume to precipitate $[Ru(pterpy)(pyterpy)][PF_6]_2$ as a red-brown powder. The FAB mass spectrum exhibits peaks at m/z 866 and 721, corresponding to $[Ru(pterpy)(pyterpy)(PF_6)]^+$ and $[Ru(pterpy)(pyterpy)]^+$ fragments, respectively. The ^1H NMR spectrum of a CD_3CN solution of the heteroleptic complex $[Ru(pterpy)(pyterpy)][PF_6]_2$ (Table 1) is very similar to a superimposition of the spectra of the homoleptic species $[Ru(pterpy)_2][PF_6]_2$ and $[Ru(pyterpy)_2][PF_6]_2$.

Though no reaction was observed to occur between equimolar quantities of $[Ru(pyterpy)Cl_3]$ and pyterpy at reflux in methanol, the reaction of hydrated ruthenium trichloride with 2 equivalents of pyterpy in boiling ethane-1,2-diol for 3 h yielded a homogeneous dark brown solution. Inspection of this crude brown reaction mixture by thin-layer chromatography [silica with acetonitrile–saturated aqueous potassium nitrate–water (7:1:0.5 v/v) as eluent] showed two minor slow-moving components in addition to a major orange species. The reaction mixture was quenched with water, and cationic species were precipitated as hexafluorophosphate salts by the addition of $[NH_4][PF_6]$. The hexafluorophosphate salts were dissolved in acetone and chromatographed on a short silica column using the same eluent system as for TLC. The orange band eluted first was collected and treated with ammonium hexafluorophosphate to give a red precipitate. This was recrystallised from acetone and methanol to give $[Ru(pyterpy)_2][PF_6]_2$ as an analytically pure red-brown microcrystalline solid in 60% yield. The FAB mass spectrum was in accord with this formulation and exhibited peaks at m/z 867 $[Ru(pyterpy)_2(PF_6)]^+$ and 722 $[Ru(pyterpy)_2]^+$ (based on ^{102}Ru). The isotopomer distributions observed were in accord with the presence of a single ruthenium atom.

The ^1H NMR spectrum of a CD_3CN solution of $[Ru(pyterpy)_2][PF_6]_2$ [Fig. 1(*b*)] was qualitatively very similar to that of the corresponding iron(II) complex [Fig. 1(*a*)]. Assignments were made on the basis of coupling constants and by analogy with other ruthenium(II) complexes of substituted 2,2′:6′,2″-terpyridine ligands. The coupling constants within the terpy group of $[Ru(pyterpy)_2][PF_6]_2$ were typical [$^3J(H^3H^4)$ 8.1, $^3J(H^4H^5)$ 7.7, $^3J(H^5H^6)$ 5.4, $^4J(H^3H^5)$ 1.2 and $^4J(H^4H^6)$ 1.4 Hz]. The pendant 4-pyridyl group appeared as an AA′MM′ multiplet with coupling constant $^3J(H_oH_m)$ 6.1 Hz typical of those measured for the iron(II) complexes and the free ligand.

We then investigated the effects of protonation of the pendant 4-pyridyl group. The addition of an excess of aqueous hexafluorophosphoric acid to an acetone–methanol (1:1) solution of $[Ru(pyterpy)_2][PF_6]_2$ resulted in a change in colour from orange to pink. Reduction in volume *in vacuo* afforded the

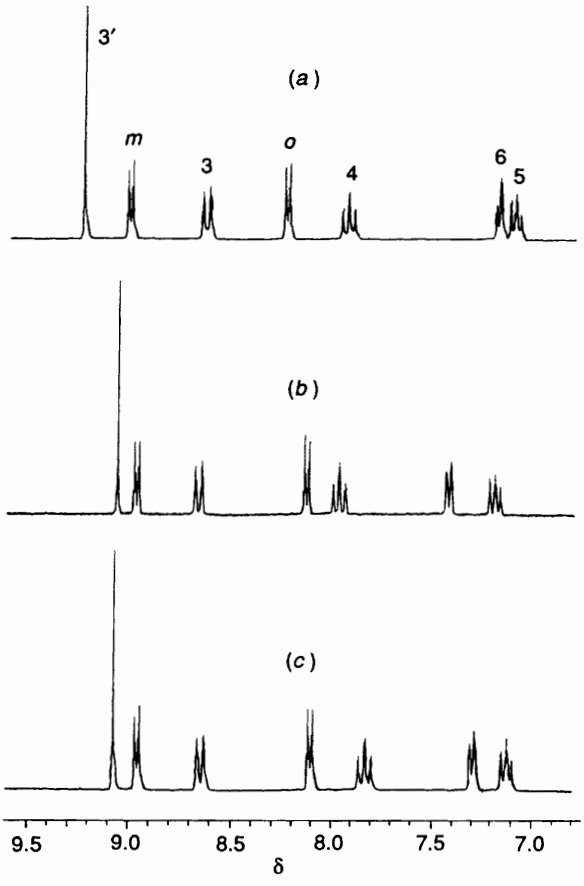

Fig. 1 The 250 MHz ^{1}H NMR spectra of CD_3CN solutions of (*a*) $[Fe(pyterpy)_2][BF_4]_2$, (*b*) $[Ru(pyterpy)_2][PF_6]_2$ and (*c*) $[Os(pyterpy)_2][PF_6]_2$

protonated complex $[Ru(Hpyterpy)_2][PF_6]_4$ as a red-brown powder. The isolation of this complex is in contrast to the behaviour of $[Fe(pyterpy)_2][PF_6]_2$, where the doubly protonated complex may only be obtained as a solution species.[4] The ^{1}H NMR spectrum of a CD_3CN solution of $[Ru(Hpyterpy)_2][PF_6]_4$ exhibited seven aromatic signals (Table 1), with H_o appearing at δ 8.74, a downfield shift of Δδ 0.60 occurring on protonation (Table 2). A similar downfield shift (Δδ 0.63) was observed for the solution species $[Fe(Hpyterpy)_2]^{4+}$. The FAB mass spectrum of $[Ru(Hpyterpy)_2][PF_6]_4$ is complicated, exhibiting peaks corresponding to the sequential loss of H and PF_6 fragments. The highest-mass peak is *m*/*z* 1013 corresponding to $[Ru(pyterpy)_2(PF_6)_2 + H]^+$.

Although the pendant pyridyl residue of $[Fe(pyterpy)_2]^{2+}$ salts reacted readily with methyl iodide to give $[Fe(mpyterpy)_2]^{4+}$ salts,[4] no such reaction was observed in acetonitrile solution between a large excess of methyl iodide and $[Ru(pyterpy)_2][PF_6]$, even after prolonged periods at 40 °C. Methylation of $[Ru(pyterpy)_2]^{2+}$ was instead achieved using trimethyloxonium tetrafluoroborate, $[Me_3O][BF_4]$. A chloroform suspension of an excess of $[Me_3O][BF_4]$ was added to an acetonitrile solution of $[Ru(pyterpy)_2][PF_6]_2$, and the resulting mixture was heated to reflux for 30 min. Inspection of the crude reaction mixture by thin-layer chromatography (silica, eluent as before) indicated that three ruthenium-containing species (orange, brown and pink) were present in solution. On the basis of the R_f values the orange complex was identified as a $[Ru(pyterpy)_2]^{2+}$ salt, the brown one as a $[Ru(pyterpy)(mpyterpy)]^{3+}$ salt and the pink species as a salt of $[Ru(mpyterpy)_2]^{4+}$. The addition of additional $[Me_3O][BF_4]$ and further reflux failed noticeably to alter the relative proportions of these three components. The reaction mixture was precipitated by the addition of an excess of ammonium hexafluorophosphate, and the brown mixture of hexafluorophosphate salts was dissolved in acetone and chromatographed upon a short silica column using the above eluent system. The first, minor orange band eluted was collected and shown to contain unreacted $[Ru(pyterpy)_2]^{2+}$ salts. The second (brown) and third (pink) components were collected separately, and pure hexafluorophosphate salts isolated as described for $[Ru(pyterpy)_2][PF_6]_2$. The complexes $[Ru(pyterpy)(mpyterpy)][PF_6]_3$ and $[Ru(mpyterpy)_2][PF_6]_4$ were obtained as red-brown analytically pure powders in 19 and 34% yields respectively. The methylated heteroleptic complex $[Ru(pterpy)(mpyterpy)]^{3+}$ was readily prepared by the same method as for $[Ru(pterpy)(pyterpy)]^{2+}$, except that an excess of MeI was added to the reaction mixture prior to isolation and chromatographic purification. The FAB mass spectra of these three methylated complexes are in accord with their proposed formulations and exhibit peaks corresponding to the sequential loss of hexafluorophosphate counter ions. The loss of the methyl groups is also observed. For example, the FAB mass spectrum of the complex $[Ru(pyterpy)(mpyterpy)][PF_6]_3$ exhibited peaks at *m*/*z* 1028, 882 and 737, corresponding to $[Ru(pyterpy)(mpyterpy)(PF_6)_n]^+$, $n = 2$, 1 and 0 respectively, as well as one at *m*/*z* 722 corresponding to $[Ru(pyterpy)_2]^+$.

The ^{1}H NMR spectrum of a CD_3CN solution of $[Ru(mpyterpy)_2][PF_6]_4$ exhibited the expected seven aromatic signals [Table 1, Fig. 2(*c*)], at near-identical chemical shifts to those observed for the protonated analogue $[Ru(Hpyterpy)_2][PF_6]_4$. The methyl group is observed as a singlet resonance at δ 4.47 {*cf.* δ 4.50 for $[Fe(mpyterpy)_2]^{4+}$}. Solutions of the monomethylated complex $[Ru(pyterpy)(mpyterpy)][PF_6]_3$ in CD_3CN exhibited fourteen aromatic resonances in their NMR spectra [Fig. 2(*b*)]. Comparison with the ^{1}H NMR spectra of $[Ru(pyterpy)_2][PF_6]_2$ and $[Ru(mpyterpy)_2][PF_6]_4$ allows unambiguous assignments of the seven resonances associated with the pyterpy ligand and the seven assigned to the mpyterpy ligand (Table 1). The methyl group was observed as a 3 H singlet at δ 4.46.

The ^{1}H NMR spectrum of a CD_3CN solution of the heteroleptic complex $[Ru(pterpy)(pyterpy)][PF_6]_2$ (Table 1) is very similar to a superimposition of the spectra of the homoleptic species $[Ru(pterpy)_2][PF_6]_2$ and $[Ru(pyterpy)_2][PF_6]_2$. We have previously reported a similar relationship for the ^{1}H NMR spectra of other homoleptic and heteroleptic ruthenium(II) bis(terpyridine) species in CD_3COCD_3.[6] Similarly, the resonances ascribable to the *N*-methylated 4′-(4-pyridyl)-2,2′:6′,2″-terpyridine ligand of $[Ru(pterpy)(mpyterpy)][PF_6]_3$ are very similar to those observed for the bis(methylated) complex $[Ru(mpyterpy)_2][PF_6]_4$.

The osmium(II) complexes $[Os(pyterpy)_2][PF_6]_2$, $[Os(Hpyterpy)_2][PF_6]_4$, $[Os(pyterpy)(mpyterpy)][PF_6]_3$ and $[Os(mpyterpy)_2][PF_6]_4$ were obtained as black solids by methods analogous to those described above for the ruthenium(II) complexes. After chromatographic separation and recrystallisation they were obtained analytically pure in 44, 84, 23 and 21% yield respectively. In acetonitrile solution, $[Os(pyterpy)_2][PF_6]_2$ is dark brown, $[Os(Hpyterpy)_2][PF_6]_4$ is purple-brown, and $[Os(pyterpy)(mpyterpy)][PF_6]_3$ and $[Os(mpyterpy)_2][PF_6]_4$ are both dark purple. In each case, the FAB mass spectrometric data were in accord with the proposed formulations, with fragments corresponding to the successive loss of $[PF_6]^-$ from the molecular ion being observed. The isotopomer distributions observed were in all cases consistent with the presence of a single osmium atom. As a typical example, the spectrum of $[Os(pyterpy)_2][PF_6]_2$ exhibited peaks centred at *m*/*z* 958 and 813, assigned to $[Os(pyterpy)_2(PF_6)]^+$ and $[Os(pyterpy)_2]^+$, respectively.

The ^{1}H NMR spectrum of a CD_3CN solution of $[Os(pyterpy)_2][PF_6]_2$ [Table 1, Fig. 1(*c*)] was very similar to that of $[Ru(pyterpy)_2][PF_6]_2$ [Fig. 1(*b*)], there being few appreciable differences in the chemical shifts of H^3, $H^{3'}$, H_o and H_m in the two complexes. Assignments were further confirmed by

Table 1 Proton NMR data (δ) for CD_3CN solutions of iron(II), ruthenium(II) and osmium(II) complexes of 2,2′:6′,2″-terpyridine and 4′-(4-pyridyl)-2,2′:6′,2″-terpyridine

Compound	H^3 (d)	H^4 (dd)	H^5 (dd)	H^6 (d)	$H^{3'}$ (d)	$H^{4'}$ (t)
terpy	8.66	7.95	7.42	8.69	8.54	8.02
$[Fe(terpy)_2][BF_4]_2$	8.47	7.87	7.06	7.06	8.91	8.68
$[Ru(terpy)_2][PF_6]_2$	8.48	7.91	7.15	7.33	8.74	8.40
$[Os(terpy)_2][PF_6]_2$	8.45	7.76	7.07	7.20	8.74	7.92

	pyterpy or *pterpy*							Hpyterpy or mpyterpy							
	H^3 (d)	H^4 (dd)	H^5 (dd)	H^6 (d)	$H^{3'}$ (s)	H_o (AB d)	H_m (AB d)	H^3 (d)	H^4 (dd)	H^5 (dd)	H^6 (d)	$H^{3'}$ (s)	H_o (AB d)	H_m (AB d)	Me (s)
pyterpy	8.72	7.99	7.47	8.74	8.80	7.83	8.77								
$[Fe(pyterpy)_2][BF_4]_2$	8.63	7.92	7.09	7.17	9.23	8.23	9.03								
$[Fe(Hpyterpy)_2]^{4+}$								8.66	7.96	7.15	7.18	9.30	8.86	9.13	
'$[Fe(pyterpy)(Hpyterpy)][PF_6]_3$'								8.64	7.95	7.11	7.19	9.27	8.54	9.07	
$[Fe(mpyterpy)_2]I_2[BF_4]_2$								8.69	7.97	7.14	7.20	9.33	8.86	9.01	4.50
$[Ru(pyterpy)_2][PF_6]_2$	8.66	7.97	7.20	7.43	9.07	8.14	8.97								
$[Ru(pterpy)_2][PF_6]_2$	*8.64*	*7.95*	*7.18*	*7.43*	*9.01*	*8.21*	*m, p 7.75(m)*								
$[Ru(Hpyterpy)_2][PF_6]_4$								8.69	8.01	7.24	7.44	9.13	8.74	9.05	
$[Ru(pyterpy)(mpyterpy)][PF_6]_3$	8.67	7.97	7.18	7.38	9.08	8.14	8.97	8.67	8.00	7.24	7.46	9.11	8.71	8.94	4.46
$[Ru(mpyterpy)_2][PF_6]_4$								8.68	8.01	7.23	7.43	9.13	8.72	8.95	4.47
$[Ru(pterpy)(pyterpy)][PF_6]_2$	*8.65*	*7.94*	*7.18*	*7.45*	*9.01*	*8.21*	*m, p 7.75(m)*								
	8.65	7.96	7.18	7.39	9.04	8.12	8.95								
$[Ru(pterpy)(mpyterpy)][PF_6]_3$	*8.66*	*7.95*	*7.16*	*7.36*	*9.04*	*8.22*	*m, p 7.75(m)*	8.69	8.00	7.25	7.50	9.10	8.73	8.94	4.47
$[Os(pyterpy)_2][PF_6]_2$	8.65	7.83	7.12	7.30	9.08	8.11	8.96								
$[Os(Hpyterpy)_2][PF_6]_4$								8.67	7.87	7.17	7.30	9.12	8.72	9.02	
$[Os(pyterpy)(mpyterpy)][PF_6]_3$	8.65	7.84	7.11	7.25	9.10	8.12	8.98	8.68	7.87	7.19	7.36	9.11	8.71	8.92	4.46
$[Os(mpyterpy)_2][PF_6]_4$								8.70	7.88	7.17	7.31	9.16	8.73	8.94	4.48

Table 2 Proton NMR co-ordination shifts (Δδ) for 2,2′:6′,2″-terpyridine and 4′-(4-pyridyl)-2,2′:6′,2″-terpyridine, and protonation and methylation shifts for 4′-(4-pyridyl)-2,2′:6′,2″-terpyridine complexes in CD_3CN solution

	Co-ordination shift, $\Delta\delta = \delta_{complex} - \delta_{free\ ligand}$					
Complex	H^3	H^4	H^5	H^6	$H^{3'}$	$H^{4'}$
$[Fe(terpy)_2][BF_4]_2$	−0.19	−0.08	−0.36	−1.63	0.37	0.66
$[Ru(terpy)_2][PF_6]_2$	−0.18	−0.04	−0.27	−1.36	0.20	0.38
$[Os(terpy)_2][PF_6]_2$	−0.21	−0.19	−0.35	−1.49	0.20	−0.10

	Co-ordination shift, $\Delta\delta = \delta_{complex} - \delta_{free\ ligand}$							Protonation/methylation shift, $\Delta\delta = \delta_{protonated/methylated\ complex} - \delta_{complex}$						
	H^3	H^4	H^5	H^6	$H^{3'}$	H_o	H_m	H^3	H^4	H^5	H^6	$H^{3'}$	H_o	H_m
$[Fe(pyterpy)_2][BF_4]_2$	−0.09	−0.07	−0.38	−1.57	0.43	0.40	0.26							
$[Fe(Hpyterpy)_2]^{4+}$								0.03	0.04	0.06	0.01	0.07	0.63	0.10
'$[Fe(pyterpy)(Hpyterpy)]^{3+}$'								0.01	0.03	0.02	0.02	0.04	0.31	0.04
$[Fe(mpyterpy)_2]I_2[BF_4]_2$								0.06	0.05	0.05	0.03	0.10	0.60	−0.02
$[Ru(pyterpy)_2][PF_6]_2$	−0.06	−0.02	−0.27	−1.31	0.27	0.31	0.20							
$[Ru(Hpyterpy)_2][PF_6]_4$								0.03	0.04	0.04	0.01	0.06	0.60	0.08
$[Ru(pyterpy)(mpyterpy)][PF_6]_3$	−0.05	−0.02	−0.29	−1.36	0.28	0.31	0.20	0.01	0.03	0.04	0.03	0.04	0.57	−0.03
$[Ru(mpyterpy)_2][PF_6]_4$								0.02	0.04	0.03	0	0.06	0.58	−0.02
$[Os(pyterpy)_2][PF_6]_2$	−0.07	−0.16	−0.35	−1.44	0.28	0.28	0.19							
$[Os(Hpyterpy)_2][PF_6]_4$								0.02	0.04	0.05	0	0.04	0.61	0.06
$[Os(pyterpy)(mpyterpy)][PF_6]_3$	−0.07	−0.15	−0.36	−1.49	0.30	0.29	0.21	0.05	0.05	0.05	0.01	0.08	0.62	−0.02
$[Os(mpyterpy)_2][PF_6]_4$								0.03	0.04	0.07	0.06	0.03	0.60	−0.04

comparison with the ^{1}H NMR spectra of $[Os(terpy)_2]^{2+}$ salts. As might be expected, the effects upon the ^{1}H NMR spectra of protonation and methylation of the osmium complex are almost identical to those observed for the corresponding ruthenium complexes. The resonance assigned to H_o of the pendant 4-pyridyl group was shifted downfield by $\Delta\delta$ 0.61 upon protonation (Table 2); very similar downfield shifts were observed for both $[Fe(Hpyterpy)_2]^{4+}$ and $[Ru(Hpyterpy)_2]^{4+}$.

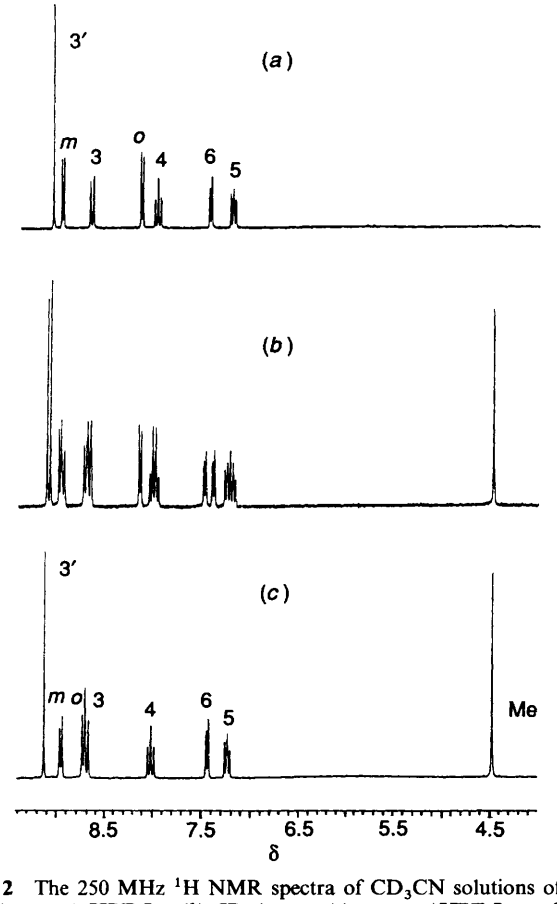

Fig. 2 The 250 MHz ^{1}H NMR spectra of CD_3CN solutions of (*a*) $[Ru(pyterpy)_2][PF_6]_2$, (*b*) $[Ru(pyterpy)(mpyterpy)][PF_6]_3$ and (*c*) $[Ru(mpyterpy)_2][PF_6]_4$

All of the complexes studied were electrochemically active in acetonitrile solution, and exhibited one fully reversible metal(II)–metal(III) redox process and two or more reversible ligand-centred reductions. These data, as well as the data for the iron(II) analogues, are presented in Table 3. The data for the analogous complexes $[M(terpy)_2][PF_6]_2$ were also determined for comparative purposes. For each of the three metals studied [iron(II), ruthenium(II) and osmium(II)], the solutions of the complex $[M(pyterpy)_2][PF_6]_2$ exhibited a metal(II)–metal(III) process at slightly more positive potentials (30–60 mV) than those observed for the corresponding $[M(terpy)_2][PF_6]_2$ complexes. This suggests that the 4-pyridyl substituent is very weakly electron withdrawing when placed in the 4' position on a 2,2':6',2''-terpyridine ligand. It can be explained in terms of the extended conjugation in pyterpy making it a better π-acceptor ligand than terpy, such that it stabilises the lower oxidation states. However, the extended conjugation is not the sole operative factor, since a phenyl substituent attached to the 4' position of a 2,2':6',2''-terpyridine is slightly electron releasing; thus $[Ru(pterpy)_2][PF_6]_2$ shows a ruthenium(II)–ruthenium(III) process at 0.895 compared to 0.92 for $[Ru(terpy)_2][PF_6]_2$ and 0.95 V for $[Ru(pyterpy)_2][PF_6]_2$.

We have previously used Hammett σ or σ^+ parameters to correlate the electronic nature of substituent groups (X, Y) in the 4' position of 2,2':6',2''-terpyridine ligands (X-terpy, Y-terpy) with the metal-centred redox potentials of the ruthenium complex cations $[Ru(X\text{-}terpy)(Y\text{-}terpy)]^{2+}$. The best correlations were obtained when σ^+ parameters were utilised.[6] This is presumably because oxidation of ruthenium(II) to ruthenium(III) results in the metal centre becoming more electron withdrawing, a situation which is better described by σ^+ than σ. Unfortunately, we have been unable to find Hammett σ or σ^+ values for 4-pyridyl substituents in the literature.[8] However, we have noted previously that these correlations were sufficiently reliable that they may be used in a predictive manner to define a Hammett σ^+ value for a substituent group X in the *para* position on an aromatic ring if the appropriate 4'-substituted 2,2':6',2''-terpyridine and its ruthenium(II) complex $[Ru(X\text{-}terpy)_2]^{2+}$ were available.[6,9] From the data (Table 4) that we have previously recorded for the six homoleptic complexes $[Ru(X\text{-}terpy)_2][PF_6]_2$ (X = H, HO, EtO, Cl, Ph or MeS), a near-linear Hammett plot of ruthenium(II)–ruthenium(III) redox potential *versus* Hammett σ^+ parameter for the substituent group X is obtained. A least-squares regression line [equation (1)] may be fitted to the data with correlation

Table 3 Redox potentials of iron(II), ruthenium(II) and osmium(II) complexes of 2,2':6',2''-terpyridine and 4'-(4-pyridyl)-2,2':6',2''-terpyridine (V, *vs.* internal ferrocene–ferrocenium; MeCN solution, $[NBu^n_4][BF_4]$ supporting electrolyte)

Complex	M^{II}–M^{III}	Reductions			
$[Fe(terpy)_2][BF_4]_2$	0.74	−1.64	−1.82		
$[Fe(pyterpy)_2][BF_4]_2$	0.80	−1.50	−1.65		
$[Fe(Hpyterpy)_2]^{4+}$	0.87	*a*			
$[Fe(mpyterpy)_2]I_2[BF_4]_2$	0.85	−1.08	−1.54		
$[Ru(terpy)_2][PF_6]_2$	0.92	−1.67	−1.92		
$[Ru(pterpy)_2][PF_6]_2$	0.895	−1.66	−1.92		
$[Ru(pyterpy)_2][PF_6]_2$	0.95	−1.54	−1.80		
$[Ru(Hpyterpy)_2][PF_6]_4$	1.045	*b*			
$[Ru(pyterpy)(mpyterpy)][PF_6]_3$	1.00	−1.09	−1.50	−1.84	
$[Ru(mpyterpy)_2][PF_6]_4$	1.03	−1.06	−1.16	−1.56	−1.79
$[Ru(pterpy)(pyterpy)][PF_6]_2$	0.89	−1.58	−1.89		
$[Ru(pterpy)(mpyterpy)][PF_6]_3$	0.945	−1.11	−1.51	−1.92	
$[Os(terpy)_2][PF_6]_2$	0.58	−1.63	−1.95		
$[Os(pyterpy)_2][PF_6]_2$	0.62	−1.47	−1.77		
$[Os(Hpyterpy)_2][PF_6]_4$	0.71	−1.11	−1.46	−1.71	
$[Os(pyterpy)(mpyterpy)][PF_6]_3$	0.68	−1.11	−1.49	−1.88	
$[Os(mpyterpy)_2][PF_6]_4$	0.74	−1.05	−1.16	−1.55	−1.88

[a] Prepared *in situ* by addition of HBF_4 to a solution of $[Fe(pyterpy)_2][BF_4]_2$; no reductions observed. [b] Reductive processes poorly resolved.

Table 4 Hammett σ^+ parameters and ruthenium(II)–ruthenium(III) potentials for $[Ru(X\text{-terpy})_2]^{2+}$ complexes

X	σ^+	$E°$/V	Ref.
HO	−0.92	0.73	6
EtO	−0.78	0.74	6
MeS	−0.60	0.80	10
Ph	−0.18	0.895	6
H	0	0.92	6
Cl	0.11	1.00	6

$$\sigma_p^+ = 4.10\,E° - 3.87 \quad (1)$$

coefficient $R^2 = 0.968$. Equation (1) may then be used to estimate the Hammett σ^+ parameter for the substituent group X from the ruthenium(II)–ruthenium(III) redox potential of the complex $[Ru(X\text{-terpy})_2]^{2+}$.

The $E°$ value of 0.95 V for the ruthenium(II)–ruthenium(III) redox potential of $[Ru(pyterpy)_2]^{2+}$ allows a σ_p^+ value for a 4-pyridyl substituent to be estimated as +0.02 using equation (1). This small positive value is in accord with the 4-pyridyl substituent being weakly electron withdrawing.

It is of note that equation (1) requires that the electrode potential, $E°$, is referenced to ferrocene–ferrocenium. Substitution of equation (2) into (1), while noting the $E°(X = H) = 0.92$ V *vs.* ferrocene–ferrocenium, gives equation (3), from which σ_p^+ can be estimated from $\Delta E°$, the *difference* between the ruthenium(II)–ruthenium(III) redox potentials of $[Ru(X\text{-terpy})_2]^{2+}$ $[E°(X)]$ and $[Ru(terpy)_2]^{2+}$ $[E°(X = H)]$, irrespective of the reference system used.

$$\Delta E° = E°(X) - E°(X = H) \quad (2)$$

$$\sigma_p^+ = 4.10\,\Delta E° - 0.10 \quad (3)$$

The complexes $[Ru(pyterpy)_2][PF_6]_2$, and $[Os(pyterpy)_2][PF_6]_2$ all exhibited two ligand-centred reductive processes. In each case they were shifted between 120 and 180 mV to potentials less negative than those for the corresponding complexes $[M(terpy)_2][PF_6]_2$. This can also be explained in terms of pyterpy being more highly conjugated than terpy, and therefore having lower-energy π^* lowest unoccupied molecular orbitals (LUMO), thus facilitating ligand-centred reductive processes. This qualitative prediction was supported by the results of Fenske-Hall self-consistent field (SCF) calculations on the free terpyridines (in the *cis,cis* conformation adopted upon chelation). The gap between the highest occupied molecular orbital (HOMO) and the LUMO dropped from 7.0 in terpy to 6.0 eV in pyterpy. Furthermore, the character of the LUMO was considerably different for the two ligands, with that of pyterpy being considerably localised on the central '4,4'-bipyridine' region (Fig. 3).

As expected, the protonation or methylation of the free 4-pyridyl ring of a co-ordinated pyterpy ligand results in the formation of a pyridinium salt with a quaternary nitrogen centre which is strongly electron withdrawing. The introduction of the strongly electron-withdrawing substituent destabilises the metal with respect to oxidation to the +III state. In the complexes containing the protonated $[M(Hpyterpy)_2]^{2+}$ cations there was a shift of the metal(II)–metal(III) process to more positive potential by 95 for ruthenium and 90 for osmium, compared to 70 mV for iron.[4] Unlike the iron(II) case for which the protonated species was only stable in solution, it was possible to isolate the salts $[Ru(Hpyterpy)_2][PF_6]_4$ and $[Os(Hpyterpy)_2][PF_6]_4$ as dark powders. The reductive processes were poorly resolved for $[Ru(Hpyterpy)_2][PF_6]_4$, but three processes were observed at −1.11, −1.46 and −1.71 V for $[Os(Hpyterpy)_2][PF_6]_4$. The increased electron-withdrawing nature of the Hpyterpy ligand results in facile ligand-centred reductive processes which are shifted to considerably less negative potentials than those for $[Os(pyterpy)_2][PF_6]_2$ (−1.47 and −1.77 V). Once again, we may use our correlation of $E°$ with σ^+ [equation (1)] to estimate the Hammett σ^+ value for a protonated 4-pyridyl substituent in the *para* position on an aromatic ring. The ruthenium(II)–ruthenium(III) potential of 1.045 V for $[Ru(Hpyterpy)_2]^{4+}$ yields a Hammett σ^+ value of +0.41. This indicates that the potonated ligand Hpyterpy is *more* electron withdrawing than is 4'-chloro-2,2':6',2''-terpytidine (cterpy) (σ^+ 0.11) but *less* electron-withdrawing than is 4'-methylsulfonyl-2,2':6',2''-terpyridine (msterpy) [for which equation (1) predicts σ^+ +0.64 given $E°$ = 1.10 V[10]]. We have demonstrated elsewhere that the electronic nature of the substitutents attached to the 4' position of such ligands allows significant control over the photophysical properties of the ruthenium complexes.[10]

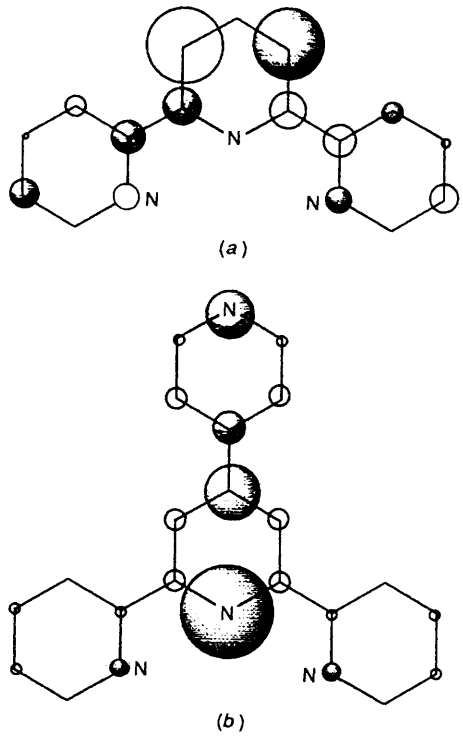

Fig. 3 Character of the LUMO of (*a*) terpy and (*b*) pyterpy as obtained from Fenske-Hall SCF calculations. The shading represents the phase of the p orbital perpendicular to and above the plane of the paper. The relative size of the orbital represents the coefficient[11]

The electronic effects of methylation of the cations $[M(pyterpy)_2]^{2+}$ are expected to be similar to those of protonation. However, the methylation reaction is such that both $[M(pyterpy)(mpyterpy)]^{3+}$ and $[M(mpyterpy)_2]^{4+}$ complexes could be isolated for the less-labile ruthenium(II) and osmium(II) cases. Whilst the iron(II)–iron(III) potential increased by 50 mV upon passing from $[Fe(pyterpy)_2]^{2+}$ to $[Fe(mpyterpy)_2]^{4+}$,[4] larger increases of 80 and 120 mV in the metal(II)–metal(III) potentials are observed for the corresponding ruthenium(II) and osmium(II) analogues respectively. The complexes $[Ru(pyterpy)(mpyterpy)][PF_6]_3$ and $[Os(pyterpy)(mpyterpy)][PF_6]_3$ had metal(II)–metal(III) potentials 50 and 60 mV, respectively, more positive than those of the parent pyterpy complexes. Thus, the additivity of parameters which we have previously described for $[Ru(X\text{-terpy})(Y\text{-terpy})]^{2+}$ complexes[6] holds for these new complexes with cationic ligands; introduction of one mpyterpy ligand was observed to have approximately half of the effect of two. The ruthenium(II)–ruthenium(III) potential in $[Ru(mpyterpy)_2][PF_6]_4$ (1.03 V) lies between that of the complex $[Ru(cterpy)_2][PF_6]_2$ which

contains the weakly electron-withdrawing ligand cterpy (1.00 V) and that of the complex of the strongly withdrawing ligand msterpy (1.10 V). This confirms that mpyterpy is a moderately electron-withdrawing ligand. A Hammett σ^+ value of +0.35 is predicted for it from the ruthenium(II)–ruthenium(III) electrode potential of 1.03 V for $[Ru(mpyterpy)_2][PF_6]_4$. The cyclic voltammogram of the heteroleptic complex $[Ru(pyterpy)(mpyterpy)][PF_6]_3$ is presented in Fig. 4.

As we noted earlier for the Hpyterpy ligand, quaternisation facilitated ligand-centred reductive processes. The complexes $[Ru(pyterpy)(mpyterpy)][PF_6]_3$ and $[Os(pyterpy)(mpyterpy)][PF_6]_3$ both exhibited three reversible reductions. In each case, the first was observed at a potential approximately 400 mV less negative than that for $[M(pyterpy)_2][PF_6]_2$. The species $[Ru(mpyterpy)_2]^{4+}$ and $[Os(mpyterpy)_2]^{4+}$ each exhibited four reductions, two of which are very significantly less negative than those of the pyterpy complexes. By contrast, the iron(II) complex $[Fe(mpyterpy)_2]^{4+}$ only exhibited two reductive waves at −1.08 and −1.54 V, although the former appeared to correspond to two overlapping one-electron processes. The half-wave separation ($E_{anodic} - E_{cathodic}$) for it (175 mV) was significantly greater than that of the iron(II)–iron(III) (110 mV) potential or that of ferrocene–ferrocenium internal reference (120 mV). It was observed, and indeed expected, that protonation and methylation of the *ligand* affected the *ligand-centred* reductive processes to a significantly larger extent than the *metal-centred* oxidation processes. It might be thought that a positively charged quaternary nitrogen centre should be more electron withdrawing than would a 4'-methylsulfonyl substituent. However, the positive charge on a protonated pyterpy ligand will be substantially localised on the quaternary nitrogen atom remote from the co-ordinated functionality, and will hence exhibit a lesser effect than if it were delocalised over the whole ligand.

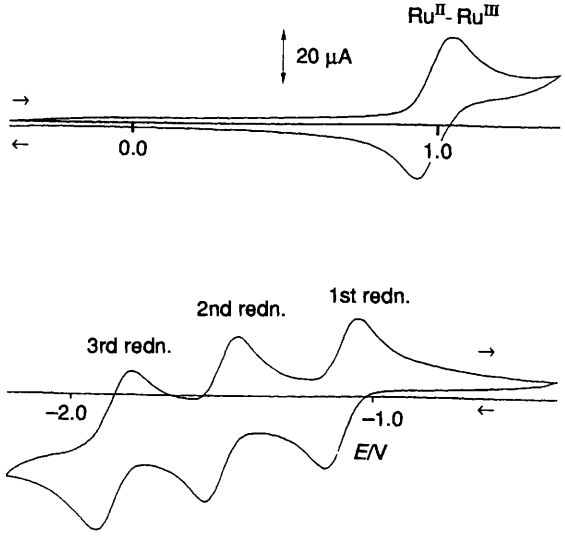

Fig. 4 Cyclic voltammogram of $[Ru(pyterpy)(mpyterpy)][PF_6]_3$ in acetonitrile solution (*vs.* ferrocene–ferrocenium)

The heteroleptic complex $[Ru(pterpy)(pyterpy)][PF_6]_2$ is oxidised reversibly at 0.89 V, and also exhibits two reductive processes within the solvent window. Methylation of the free pyridyl ring to give $[Ru(pterpy)(mpyterpy)][PF_6]_3$ results in the ruthenium(II)–ruthenium(III) potential being shifted by 55 mV to 0.945 V. As expected, this is very similar to the shift of 50 mV observed upon monomethylation of $[Ru(pyterpy)_2][PF_6]_2$.

Electronic spectra were recorded in the range 200–750 nm for acetonitrile solutions of all of the complexes. The wavelengths of the peaks at maximum intensity and their absorption coefficients are given in Table 5. Data for the $[M(terpy)_2][PF_6]$ complexes are presented for comparison, as are those for pyterpy. As for the iron(II) complexes, the most interesting feature in the electronic spectra of the ruthenium(II) and osmium(II) species was the intense metal-to-ligand charge-transfer (m.l.c.t.) transition in the visible region. These peaks were broad and asymmetric, and the m.l.c.t. absorption is responsible for the vivid colours of the complexes. The complexes also exhibited various ligand-centred $\pi^* \longleftarrow \pi$ and $\pi^* \longleftarrow n$ transitions at higher energy. One absorption in the range λ_{max} 310–335 nm tended to be affected significantly by protonation or methylation of the ligand. One or more shoulders of moderate intensity were usually observed to low energy of this transition, and were best observed in the spectra of the protonated and methylated species. One absorption occurred in the range λ_{max} 270–286 nm, another in the range λ_{max} 238–259 nm. None of these transitions was significantly affected by protonation or methylation, nor did they vary with the metal present. Similar transitions at λ_{max} 310, 276 and 240

Table 5 Electronic spectroscopic data for iron(II), ruthenium(II) and osmium(II) complexes of 4'-(4-pyridyl)-2,2':6',2''-terpyridine

Compound	λ_{max}/nm ($\varepsilon/10^3$ dm^3 mol^{-1} cm^{-1})					
pyterpy			310 (6.8)	276 (24.2)[a]		240 (37.8)
$[Fe(terpy)_2][BF_4]_2$		551 (11.6)	318 (51.8)	280 (33.7)	272 (38.7)	
$[Fe(pyterpy)_2][BF_4]_2$		569 (24.5)	324 (41.6)	284 (72.0)	276 (64.1)	245 (39.4)
$[Fe(Hpyterpy)_2]^{4+}$ [b]		594	335	282[a]		239
$[Fe(mpyterpy)_2]I_2[BF_4]_2$		595 (25.7)	330 (25.2)	286 (60.5)	278 (55.9)	247 (41.7)
$[Ru(terpy)_2][PF_6]_2$		475 (11.6)	307 (52.4)		270 (31.6)	
$[Ru(pyterpy)_2][PF_6]_2$		488 (30.9)	312 (61.6)		273 (78.4)	238 (43.5)
$[Ru(Hpyterpy)_2][PF_6]_4$		502 (40.5)	313 (37.7)		273 (93.0)	238 (55.8)
$[Ru(pyterpy)(mpyterpy)][PF_6]_3$		500 (30.3)	313 (45.3)		275 (77.2)	240 (44.6)
$[Ru(mpyterpy)_2][PF_6]_4$		507 (39.8)	313 (35.3)		276 (81.6)	240 (51.2)
$[Ru(pterpy)(pyterpy)][PF_6]_2$		488 (28.8)	311 (62.5)		275 (71.8)	238 (37.5)
$[Ru(pterpy)(mpyterpy)][PF_6]_3$		503 (30.5)	310 (49.5)		276 (76.7)	240 (41.0)
$[Os(terpy)_2][PF_6]_2$	656 (4.2)	475 (15.4)	310 (74.2)		270 (43.9)	229 (41.9)
$[Os(pyterpy)_2][PF_6]_2$	668 (7.3)	486 (29.4)	315 (64.4)		275 (71.8)	238 (43.6)
$[Os(Hpyterpy)_2][PF_6]_4$	689 (8.5)	500 (37.0)	323 (46.1)		275 (73.0)	238 (48.5)
$[Os(pyterpy)(mpyterpy)][PF_6]_3$	681 (6.9)	496 (33.4)	315 (50.7)		276 (73.7)	238 (45.1)
$[Os(mpyterpy)_2][PF_6]_4$	693 (10.7)	504 (44.4)	326 (45.5)		276 (77.4)	238 (50.3)

[a] Broad peak. [b] The ε values could not be measured as $[Fe(Hpyterpy)_2]^{4+}$ was prepared as a solution species.

nm were also observed for acetonitrile solutions of the free pyterpy (Table 5), strongly suggesting that the analogous transitions in the complexes were also ligand centred. The electronic spectrum of free pyterpy is very similar to that reported for the comparable pterpy.

The orange complex $[Ru(pyterpy)_2][PF_6]_2$ had the lowest-energy m.l.c.t. transition at λ_{max} 488 nm (ε 30 900 dm^3 mol^{-1} cm^{-1}). Again, this transition was at a lower energy and was considerably more intense than that for $[Ru(terpy)_2][PF_6]_2$ (λ_{max} 475 nm, ε 11 600 dm^3 mol^{-1} cm^{-1}). An increase in conjugation can again be invoked to explain both the bathochromic shift to lower energy due to the lowering of the ligand π^* orbitals, and the increase in absorption coefficient. The ligand pterpy might be expected to be a better model for pyterpy than the less-conjugated parent terpy. This was borne out by the observation that $[Ru(pterpy)_2][PF_6]_2$ exhibited λ_{max} 488 nm (ε 26 000 dm^3 mol^{-1} cm^{-1}).[6] As with the iron complexes, protonation and methylation both resulted in shifts to lower energy, with corresponding changes in the colour of acetonitrile solutions. The pink fully protonated species $[Ru(Hpyterpy)_2][PF_6]_4$ has λ_{max} 502 nm (ε 40 500 dm^3 mol^{-1} cm^{-1}), whilst brown $[Ru(pyterpy)(mpyterpy)][PF_6]_3$ and pink $[Ru(mpyterpy)_2][PF_6]_4$ had λ_{max} 500 (ε 30 300) and 507 nm (ε 39 800 dm^3 mol^{-1} cm^{-1}), respectively. Although there was little change in the energy of the ligand-centred transition at λ_{max} 312 nm on protonation or methylation, there was a significant drop in its intensity. The similarity between the electronic spectra of $[Ru(pyterpy)_2][PF_6]_2$ and $[Ru(pterpy)_2][PF_6]_2$ has already been noted. It is not, therefore, surprising that the electronic spectrum of the heteroleptic complex $[Ru(pterpy)(pyterpy)][PF_6]_2$ is very similar to the spectra of these homoleptic species, with the main m.l.c.t. transition occurring at λ_{max} 488 nm (ε 28 800 dm^3 mol^{-1} cm^{-1}). As might also be expected, the electronic spectrum of the brown methylated species $[Ru(pterpy)(mpyterpy)][PF_6]_3$ (λ_{max} 503 nm, ε 30 500 dm^3 mol^{-1} cm^{-1}) is very similar to that of $[Ru(pyterpy)(mpyterpy)][PF_6]_3$.

In general, osmium(II) bis(terpyridine) complexes exhibit very similar electronic spectra to their ruthenium(II) analogues, as can be seen in the data presented for $[Os(terpy)_2][PF_6]_2$ and $[Ru(terpy)_2][PF_6]_2$ (Table 5). The electronic spectra of the osmium(II) complexes of pyterpy studied were almost identical to those of their ruthenium(II) counterparts, except that they exhibited an additional low-energy m.l.c.t. transition of low intensity ($\varepsilon \approx 10\,000$ dm^3 mol^{-1} cm^{-1}) in the range λ_{max} 668–693 nm. It is this triplet state that is responsible for the room-temperature luminescence of osmium(II) bis(terpyridine) centres in many cases.[12] As expected, protonation or methylation of the ligand both shifted this transition to lower energy, while increasing its intensity. For example, $[Os(pyterpy)_2][PF_6]_2$ had λ_{max} 668 nm (ε 7300 dm^3 mol^{-1} cm^{-1}), while $[Os(mpyterpy)_2][PF_6]_4$ had λ_{max} 693 nm (ε 10 700 dm^3 mol^{-1} cm^{-1}). The electronic spectra of $[Ru(mpyterpy)_2][PF_6]_4$ and $[Os(pyterpy)_2][PF_6]_2$ are presented in Fig. 5.

In conclusion, the protonation or methylation of the remote non-co-ordinated pyridyl nitrogen atom of a co-ordinated 4'-(4-pyridyl)-2,2':6',2''-terpyridine ligand allows subtle but significant changes to be made to the redox and photophysical properties of the co-ordination complex as a whole.

We are currently using the relationship (1) to assign Hammett σ^+ values to novel substituent groups in the 4' positions of 2,2':6',2''-terpyridine ligands. We are also determining whether similar relationships can be devised for $[Fe(X\text{-}terpy)_2][PF_6]_2$ and $[Os(X\text{-}terpy)_2][PF_6]_2$ systems, and are investigating the photophysical properties of the complex $[Ru(mpyterpy)_2][PF_6]_4$ in collaboration with Professor Balzani in Bologna. The electron-withdrawing ligand mpyterpy is expected to render the ruthenium(II) centre to which it is co-ordinated luminescent at room temperature, as we have observed[10] for the complexes $[Ru(cterpy)_2][PF_6]_2$ and $[Ru(msterpy)_2][PF_6]_2$.

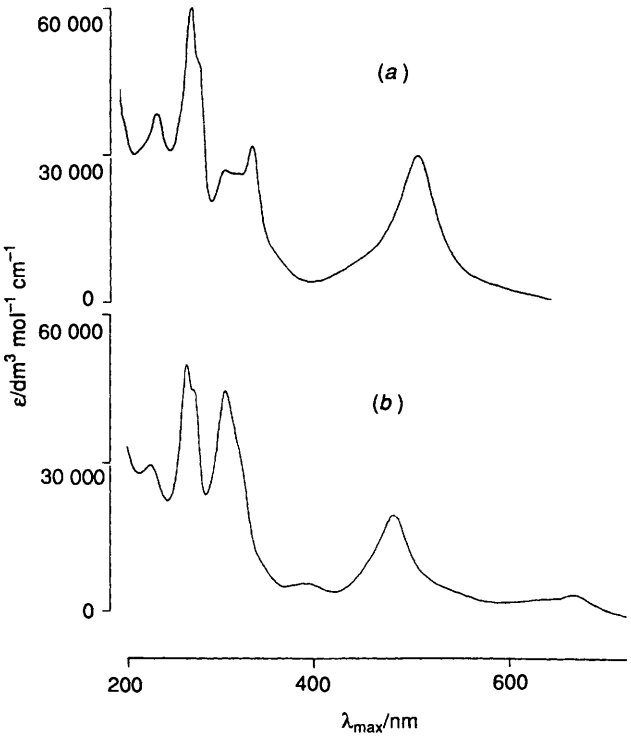

Fig. 5 Electronic spectra of acetonitrile solutions of (*a*) $[Ru(mpyterpy)_2][PF_6]_4$ and (*b*) $[Os(pyterpy)_2][PF_6]_2$

Acknowledgements

We thank the SERC for a studentship (to A. M. W. C. T.), the Royal Society of Great Britain (E. C. C.) and the Isaac Newton Trust (E. C. C.) for support; this research is currently supported by the Schweizerischer Nationalfonds zur Förderung der Wissenschaftlichen Forschung (Grant number: 21-37325.93). We also thank Dr. C. E. Housecroft for assistance in the use of the Fenske-Hall program.

References

1 E. C. Constable, *Prog. Inorg. Chem.*, in the press; *Chem. Ind.*, 1994, 56.
2 E. C. Constable, A. J. Edwards, P. R. Raithby and J. V. Walker, *Angew. Chem.*, 1993, **32**, 1465 and refs. therein.
3 E. C. Constable, A. M. W. Cargill Thompson and S. Greulich, *J. Chem. Soc., Chem. Commun.*, 1993, 1444 and refs. therein.
4 E. C. Constable and A. M. W. Cargill Thompson, *J. Chem. Soc., Dalton Trans.*, 1992, 2947.
5 E. C. Constable, A. M. W. Cargill Thompson and D. A. Tocher, *Polym. Preprints*, 1993, **34**, 110; *Makromol. Chem.*, in the press; E. C. Constable, A. M. W. Cargill Thompson and D. A. Tocher, *Supramol. Chem.*, 1993, **3**, 9.
6 E. C. Constable, A. M. W. Cargill Thompson, D. A. Tocher and M. A. M. Daniels, *New J. Chem.*, 1992, **16**, 855.
7 E. C. Constable, *Adv. Inorg. Chem. Radiochem.*, 1986, **30**, 69 and refs. therein.
8 C. Hansch, A. Leo, S. Unger, K. H. Kim, D. Nikaitani and E. J. Liem, *J. Med. Chem.*, 1973, **16**, 1207; H. C. Brown and Y. Okamato, *J. Am. Chem. Soc.*, 1958, **80**, 4979; C. D. Ritchie and W. F. Sagar, *Prog. Phys. Org. Chem.*, 1964, **2**, 323.
9 E. C. Constable, A. J. Edwards, R. Martínez-Máñez, P. R. Raithby and A. M. W. Cargill Thompson, *J. Chem. Soc., Dalton Trans.*, 1994, 645.
10 E. C. Constable, A. M. W. Cargill Thompson, N. Armaroli, V. Balzani and M. Maestri, *Polyhedron*, 1992, **11**, 2707.
11 See: E. C. Constable and C. E. Housecroft, *Polyhedron*, 1990, **9**, 1939; M. B. Hall and R. F. Fenske, *Inorg. Chem.*, 1972, **11**, 768.
12 S. Campagna, G. Denti, L. Sabatino, S. Serroni, M. Ciano and V. Balzani, *J. Chem. Soc., Chem. Commun.*, 1989, 1500.

Received 2nd December 1993; *Paper* 3/07133B